

# Influence of Climatic Ageing on the Mechanical Properties and the Microstructure of Low-Density Polyethylene Films

S. F. Chabira,<sup>1</sup> M. Sebaa,<sup>1</sup> C. G'sell<sup>2</sup>

<sup>1</sup>Laboratoire de Rhéologie des Polymères, Université Ammar Telidji, BP 37 G, Laghouat 03000, Algérie

<sup>2</sup>Laboratoire de Physique des Matériaux (UMR 7556 CNRS-INPL-UHP), Nancy-Université, Ecole des Mines, Parc de Saurupt, Nancy 54042, France

Received 11 December 2007; accepted 2 June 2008

DOI 10.1002/app.28823

Published online 20 August 2008 in Wiley InterScience (www.interscience.wiley.com).

**ABSTRACT:** Blown extruded films of low-density polyethylene (LDPE) have been subjected to climatic ageing in a sub-Saharan facility at Laghouat (Algeria) with direct exposure to sun. Samples were characterized by complementary techniques after prescribed amounts of time up to 8 months. It was shown by tensile testing that the mechanical properties are quite sensitive to ageing: (i) the elastic modulus increases and saturates, (ii) the tensile stress increases slightly, and (iii) the rupture energy decreases dramatically after 4 months weathering. Fourier-transform infrared spectroscopy (FTIR) and nuclear magnetic resonance (<sup>13</sup>C NMR) were performed to identify the evolution of the polymer microstructure. The FTIR spectra reveal the initial presence of vinylidene groups that exhaust rapidly after 4 months ageing. Also, it detects the progressive multiplication of vinyl groups and oxidation products of many kinds. The NMR technique revealed specif-

ically the carbon-carbon configurations in the polymer chains. By contrast to the original film that contained almost exclusively butyl chain branches, the aged specimens presented shorter ramifications, namely ethyl branches. Also, the presence of quaternary atoms was detected after long ageing times. The discussion of these complementary results in the light of current literature makes possible to identify the leading mechanisms that control the decay of LDPE film properties. Although these mechanisms are numerous and complex, they can be schematically summarized within three main classes: oxidation, scission, and crosslinking. Each class is discussed in details. © 2008 Wiley Periodicals, Inc. *J Appl Polym Sci* 110: 2516–2524, 2008

**Key words:** low-density polyethylene; climatic ageing; mechanical properties; <sup>13</sup>C NMR; FTIR

## INTRODUCTION

The use of low-density polyethylene (LDPE) films for greenhouse covering increased considerably during the past decade, particularly in the agricultural sub-Saharan regions. This is because this type of agriculture allows earlier production, higher yields, and sustainable water economy. However, in such regions where sun irradiation is very intensive, it was reported by several authors that the films undergo rapid degradation when exposed outdoor to climatic ageing.<sup>1–4</sup> The effect of sun exposure was also investigated for other polyethylene grades, like linear LDPE<sup>4</sup> and high-density polyethylene.<sup>5</sup>

Although the study of UV-irradiation ageing in accelerated tests with artificial sources requires less time due to constant photon flux and faster degradation kinetics,<sup>6,7</sup> it is important to study the climatic ageing phenomena in outdoor experiments as well. This is because natural weathering represents a complex combination of factors including sun radiation

periodicity, temperature, humidity, sand wind stresses, and atmospheric gases permeation (oxygen and pollutants).<sup>8</sup> The effect of these factors intervening altogether cannot be predicted simply by the combination of results from standard laboratory tests for which environmental constraints are imposed separately.<sup>9,10</sup>

In spite of the great research effort devoted to elucidate the complex chemical mechanisms that control polyethylene degradation,<sup>11–15</sup> more experimental characterization and reaction modeling is required to understand definitely the interaction between polymeric chains, energetic photons, and atmospheric oxygen.

This work completes previous analyses performed by two of us<sup>16,17</sup> in which the research was focused on the evolution of anisotropic ultrasonic propagation in weathered LDPE films. Here, we investigate again the case of films subjected to climatic ageing, and we aim interpreting the effect of degradation mechanisms on the mechanical properties under uniaxial tension. In that scope aged samples were systematically analyzed by three microstructural characterization methods: calorimetric tests (DSC), infrared spectroscopy, and nuclear magnetic resonance (<sup>13</sup>C NMR).

Correspondence to: S. F. Chabira (s.chabira@mail.lagh-univ.dz).

## MATERIAL AND METHODS

### Material and ageing conditions

The LDPE utilized in this investigation is a commercial film produced by the ENIP Company, Skikda, Algeria under the reference: B24/2. This polymer is a neat grade exempt of stabilizing agents. The melt was extruded at about 175°C and blown in a continuous process characterized by a bubble diameter of 4.4 m, a wall thickness of 180 μm, and a drawing speed of 15 cm/s.

Film cuts were mounted within wooden frames facing south, inclined at 45°, according to the standard NF T51-165. The solar exposure took place at Laghouat, Algeria (38° 48' N) from October to June. The maximum time of 8 months corresponds to the time at which the films became too brittle to resist to the wind force.

Samples were picked up periodically, during all the ageing period, from film zones sufficiently far away from the contact points with the holding frame. This precaution was taken to avoid uncontrolled overheating of the material: although the maximum temperature attained in the material reaches about 48°C under solar exposure where the film is free, temperatures as high as 70°C may be attained in the portions of the film that are in contact with metallic or wooden structures, as reported in the literature.<sup>9,10,18,19</sup>

### Mechanical testing

Tensile tests were run with an Instron 4464 machine accordingly to the NF T54-102 standard with rectangular specimens cut out of the original and aged films. The dimensions of the test pieces were 180 mm × 10 mm, with a calibrated portion of length  $L_0 = 120$  mm, width  $W_0 = 10$  mm, and thickness  $T_0 = 0.18$  mm. All the tests were conducted at room temperature ( $T = 21^\circ\text{C} \pm 1^\circ\text{C}$ ) at a nearly constant relative humidity (RH = 50% ± 5%). According to the NF standard, the results of the tensile test are presented in terms of the nominal stress,  $\sigma = F/(W_0 \times T_0)$  and the nominal strain,  $\varepsilon = L/L_0 - 1$ , where  $L$  is the current length of the calibrated portion of the sample and  $L_0$  is the initial length. The Young's modulus ( $E$ ) was determined as the initial slope of the  $\sigma(\varepsilon)$ .

It should be noted that the definitions of nominal stress and strain are merely conventional. In the case of neat LDPE, it is well known that necking appears while the specimen is stretched because of the low strain-hardening of the polymer. Consequently, the material behavior would be better described in principle by the true stress-strain behavior. Although one of us (C.G.) is specialized in such problems, we were decided to keep the standard NF protocol for

several reasons: (i) the automatic monitoring of local thickness variations is very difficult in film specimens, (ii) the deformation is homogeneous in the elastic range so that the nominal Young's modulus is quite precise, (iii) the neck formed after the yield point propagates over the entire specimen length so that the discrepancy between true and nominal stress becomes very small at rupture, and (iv) the necking process becomes less and less visible as the solar irradiation time is increased and the local stress analysis loses its pertinence.

To optimize the duration of the tests, the strain rate was fixed at a low value to the yield point ( $d\varepsilon/dt = 3 \times 10^{-4} \text{ s}^{-1}$ ) and then stepped to a higher value ( $d\varepsilon/dt = 3 \times 10^{-2} \text{ s}^{-1}$ ) for the rest of the test until fracture occurred. The stress and strain at rupture ( $\sigma_r$ ,  $\varepsilon_r$ ) were measured while the sample reached its ultimate elongation before ductile or semibrittle failure occurred.

### Microstructural characterization

The degree of crystallinity of the samples was determined in the standard way from the heat of fusion  $\Delta H_f$  by means of a differential scanning calorimeter (DSC Mettler TA 3000) interfaced to a microcomputer controller. Indium was used for calibration. The samples (about 10 mg in weight) were heated from  $-150$  to  $200^\circ\text{C}$  with a heating rate of  $10^\circ\text{C}/\text{min}$ . The mass-based degree of crystallinity was calculated with reference to the thermodynamic heat of fusion of 100% crystallized polyethylene ( $\Delta H_f^c = 285 \text{ J/g}^{20}$ ) by the relationship:  $X_c^m = \Delta H_f / \Delta H_f^c$ .

Infrared spectroscopy was performed on an FTIR apparatus "Nicolet 210 in. (now maintained by Brücker). The specific absorption peaks were analyzed from the spectra delivered by the equipment. For each peak the "optical density" (OD) was determined following the usual definition as:  $\text{OD} = \ln(I_0/I)$ , where  $I_0$  is the reference infrared intensity corresponding to the baseline of the spectrum at the peak wave number and  $I$  is the minimum intensity at the base of the peak.

NMR spectra were acquired with a high-resolution  $^{13}\text{C}$  Brücker DPX apparatus, operating at a frequency of 400 MHz. The specimen glass tube introduced in the apparatus contained a few milligrams of the LDPE films dissolved in deuterated ethylene tetrachloride ( $\text{C}_2\text{D}_2\text{Cl}_4$ ) at  $110^\circ\text{C}$ . To distinguish the parity of bonds of carbon atoms, we completed the conventional NMR investigation with the standard Attached Proton Test (APT).<sup>21</sup> In this procedure, the NMR peaks due to evenly bonded atoms (C and  $\text{CH}_2$ ) remain positive, whereas those due to oddly bonded atoms (CH and  $\text{CH}_3$ ) become negative.

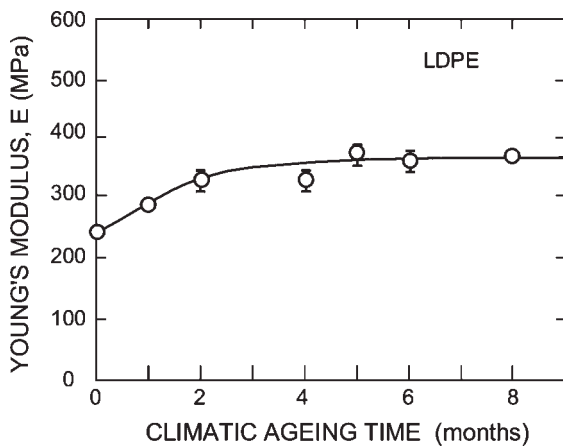


**Figure 1** Evolution of the Young's modulus ( $E$ ) of the LDPE films during climatic ageing.

### EVOLUTION OF THE MECHANICAL PROPERTIES

The graph in Figure 1 shows the variations of the Young's modulus,  $E$ , versus climatic ageing time. The evolution of  $E$  is not monotonous: after a fast initial increase, the modulus saturates at 350 MPa after 3 months ageing.

The variations of the rupture stress ( $\sigma_r$ ) reported versus ageing time in Figure 2 are characterized by: (i) an initial plateau during 3 months, (ii) a dramatic drop of about 35% with a minimum at about 5 months, and (iii) a final consolidation.

Whatever the importance of the above curves, the most dramatic evolution shown in the mechanical properties is that of the deformation at rupture that is directly sensitive to the evolution of the polymer microstructure under the effect of the climatic ageing. The  $\varepsilon_r$  versus ageing time that are displayed in Figure 3 show that the maximum strain attained by the sample decreases dramatically from 500% to

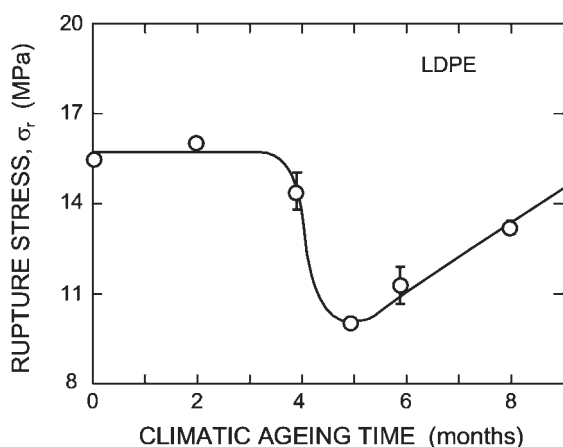


**Figure 2** Evolution of the rupture stress ( $\sigma_r$ ) of the LDPE films during climatic ageing.

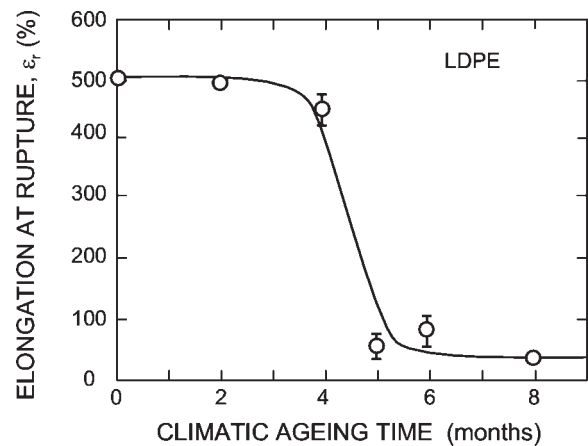


**Figure 3** Evolution of the elongation at rupture ( $\varepsilon_r$ ) of the LDPE films during climatic ageing.

about 20%. It is seen that the ductile-to-brittle transition occurs at about 4.5 months.

### EVOLUTION OF THE POLYMER MICROSTRUCTURE

#### Polymer crystallinity

The graph of Figure 4 shows that the degree of crystallinity, that is originally weak in the LDPE under investigation ( $X_c^m = 36\%$ ), increases significantly with climatic ageing time. Because in the experimental conditions the holding temperature is far below the fusion peak (which begins at about 60°C in this grade), it should be considered that the increase of  $X_c^m$  is due to the secondary crystallization of short chain segments that acquired sufficient mobility for being incorporated in existing lamellae or to nucleate new crystallites.<sup>14</sup> It is interesting to note that the increase of crystallinity is accompanied by a limited, but significant, thickening of the crystalline lamellae.

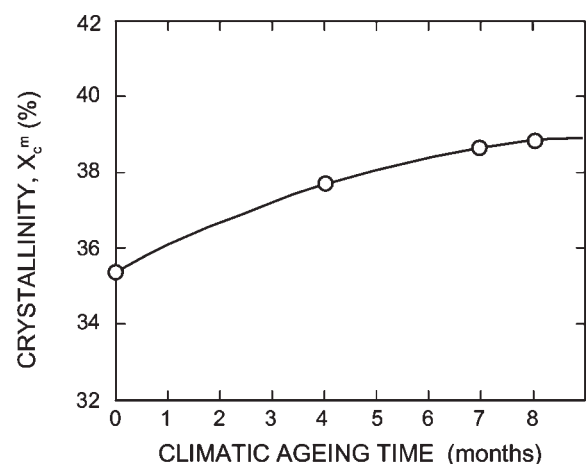


**Figure 4** Evolution of the crystallinity ( $X_c^m$ ) of the LDPE films during climatic ageing.

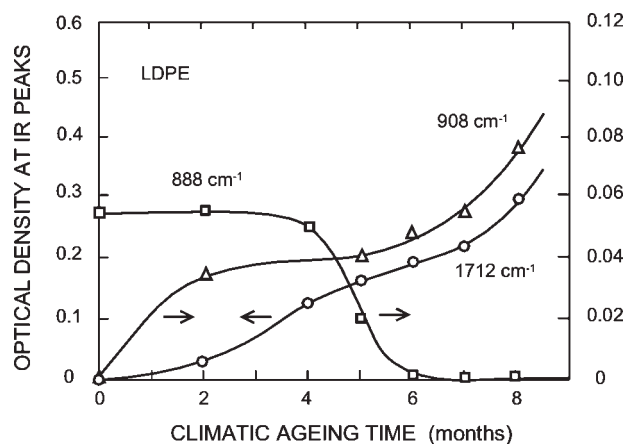


**Figure 5** Optical density (OD) of the infrared peaks at  $888\text{ cm}^{-1}$ ,  $908\text{ cm}^{-1}$ , and  $1712\text{ cm}^{-1}$ .

The melting temperature recorded in the DSC experiments at the top of the fusion peak increases with the ageing time:  $116.6^{\circ}\text{C}$  for the original films,  $117.5^{\circ}\text{C}$  after 4 months ageing, and  $119.3^{\circ}\text{C}$  after 8 months. Applying the classical Gibbs-Thomson model with the characteristic thermodynamic parameters of polyethylene published earlier (e.g., Wunderlich<sup>20</sup>), we find that the most probable thickness of the lamellae, which is equal to 10.5 nm in the original state, increases to 10.9 nm after 4 months ageing and 11.7 nm after 8 months.

It is evident that the variations of the Young's modulus (Fig. 1) and that of crystallinity (Fig. 4) are correlated:  $E$  and  $X_c^m$  increase in both cases during the first period of the climatic ageing and then saturate after 3 months ageing. This result is in line with previous studies presented in the literature stating that the stiffening of polyethylene comes from a major part from the increase of crystallinity.<sup>6</sup> Also, it was already shown that, in LDPE, the secondary crystallization of low molecular weight chains is fairly rapid at temperatures above  $T_g$ .<sup>22</sup>

### FTIR characterization

The infrared spectra obtained in this work with the original and aged LDPE films are identical to those presented previously by two of us.<sup>17</sup> We will analyze below more quantitatively the three bands at  $888\text{ cm}^{-1}$ ,  $908\text{ cm}^{-1}$ , and  $1712\text{ cm}^{-1}$  from the plots in Figure 5 that represent the optical density (OD) of each band versus the climatic ageing time.

The absorption band at  $888\text{ cm}^{-1}$  characterizes the vinylidene groups ( $\text{CH}_2$  side group linked to the polyethylene skeleton by a double bond). This unsaturated configuration, which does not correspond to the nominal microstructure of LDPE, appears during the high-pressure polymerization process.<sup>1</sup> Figure 5 shows that the population of the vinylidene species decreases during the ageing process.

The bands at  $908\text{ cm}^{-1}$  is due to vinyl groups ( $\text{CH}_2$  group linked to a  $\text{CH}$  group at the end of a chain by a double bond). These groups are not present in the microstructure of the original films. They appear progressively during the climatic ageing.

Finally the band at  $1712\text{ cm}^{-1}$  has a complex structure. Basically, it corresponds to the carbonyl group (side oxygen linked to a carbon atom of the chain by a double bond). It is thus characteristic of the reaction of the LDPE with atmospheric oxygen. In fact, several groups involve the presence of a carbonyl group, which contribute to the broad band around  $1712\text{ cm}^{-1}$  by shoulders that are difficult to analyze separately. Among these configurations, the literature [e.g., Ref. 15] reports the occurrence of carboxylic acids, esters, peresters, peracids, etc. After a short induction period, it is visible in Figure 5 that the optical density of this band increases dramatically during climatic ageing, proving the progressive oxidation of the polymer.

### NMR characterization

The  $^{13}\text{C}$  NMR spectrum of a film after 8 months of climatic ageing is displayed in Figure 6. It is exactly identical to that obtained with the initial film, except that new resonances appeared at shifts of 38.81 ppm, 26.69 ppm, and 11.07 ppm, whose intensities are very weak. We will identify firstly the main peaks of the polymer based on the relevant literature.<sup>23–28</sup> Subsequently, we will analyze the three extra peaks.

The microstructure of the LDPE under investigation is characterized by the presence of many short chain branches (SCB) grafted on the main polyethylene skeleton. The NMR spectrum of the original films provides several indications that these branches have principally the butyl structure (four carbon atoms) depicted by the simplified model in Figure 7: (i) the peak at 14.08 ppm is due to the methyl carbon (1S) at the end of the butyl branch, (ii) the peak at 38.08 ppm is due to the methine carbon ( $\text{C}^{\text{br}}$ ) to which the branch is attached, (iii) the peaks at 23.25 ppm and at 34.07 ppm are due to the 2S and 4S carbons,

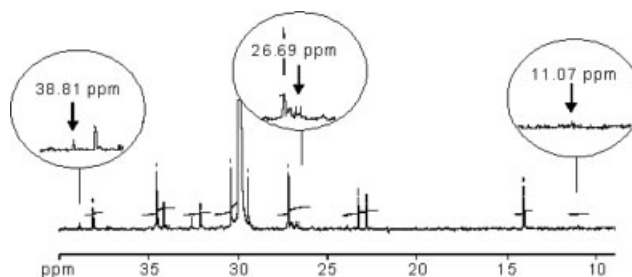


**Figure 6**  $^{13}\text{C}$  NMR spectrum of a LDPE film after 8 months of climatic ageing. The three peaks in the round inserts were not visible in the initial state.

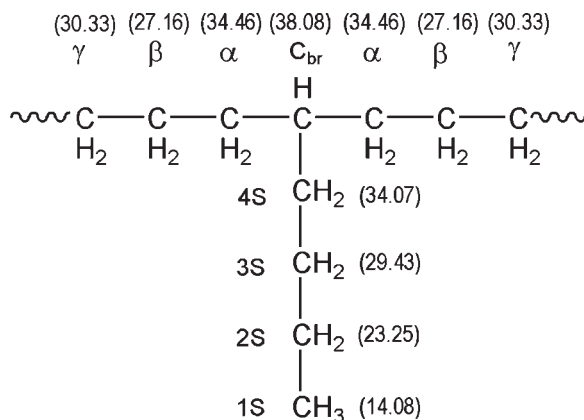


**Figure 7** Microstructure of an adjacent butyl branch in polyethylene.

respectively, and (iv) the peaks at 34.46 ppm, 27.16 ppm, and 30.33 ppm are due to the carbon atoms neighboring  $C^{br}$  in the skeleton (atoms  $\alpha$ ,  $\beta$ , and  $\gamma$ , respectively). Concerning the latter peaks, they have almost the same intensity that is twice the intensity of the branch carbons. These remarks support the assumption that they do belong to the main chain.<sup>28</sup>

To a lower extent, amyl branches are also identified (5 carbon atoms). The peaks at 22.75 ppm and 32.57 ppm are generally attributed to the 2S and 3S carbon of an amyl branch. The resonances lines of the methine carbon ( $C^{br}$ ) and the methyl carbon (1S) of the amyl branch are overlapped with those of the butyl branch. The weak resonance at 26.74 ppm is that of the carbon 4S. The carbon in the  $\alpha$  position to  $C^{br}$  is overlapped with that of the butyl branch.

It is probable that this LDPE does not contain long chain branches (LCB) or, if any, in very small proportions. This is proved by the fact that no peak is detected in the NMR spectra at the shifts 36.2 ppm, 32.6 ppm, and 25.3 ppm that correspond in a LCB configuration to  $C^{br}$ ,  $\alpha$ , and  $\beta$  carbons, respectively. If such LCB would exist, they would be themselves branched with short chain branches.

Let us now examine the three peaks that appeared on ageing. The use of the APT procedure helps to assign them to specific carbon bonding configurations. It was found that the signals of the peaks at 38.81 ppm and 26.69 ppm remained positive when analyzed by APT. By contrast, the signal for the

11.07 ppm became negative. In agreement with previous authors,<sup>24,25</sup> this investigation proves that the NMR peaks in question correspond to the following configurations: quaternary carbon atoms (C) for 38.81 ppm, 2S carbon atoms ( $CH_2$ ) for 26.69 ppm, and 1S carbon atoms ( $CH_3$ ) for 11.07 ppm.

## DISCUSSION

### Macromolecular processes induced by climatic ageing

On the basis of the above results and of models presented previously in the literature, we present in this section a review of the different molecular mechanisms that are activated in the polyethylene films under the effect of sun radiation, temperature, and atmospheric oxygen. This description is necessarily simplified but it should rather be considered as a step towards a comprehensive model. As we will show, the main effects can be classified into three categories, namely: (i) oxidation, (ii) chain scission, and (iii) crosslinking. For each category the possible reactions will be presented and discussed.

The UV-irradiation in the wavelength range between 290 and 400 nm is absorbed by the material. The initial presence of structural defects leads to the formation of polymer free radicals and macropoxy radicals. Bond cleavage and depolymerization cause the photodegradation of the material.<sup>29</sup> The characterization of molecular weight distribution was not performed in this work because its results should have been identical to those published elsewhere.<sup>1,3</sup> It was shown in the latter references that climatic ageing of LDPE provokes the gradual decrease of the average molecular weight together with the marked widening of the (Gaussian) molecular weight distribution. It is easily shown that these two features correspond to the gradual decrease of long polymeric chains population. These chains being mainly responsible of the polymer toughness, their scission induce the progressive embrittlement of the films.

The free radicals created by hydrogen abstraction (Fig. 8) can *a priori* be formed at diverse sites of the polymer chains. For example they can occur at the root of a lateral branch ( $C^{br}$  atom), at any site along the LDPE chain via the reaction with a free radical

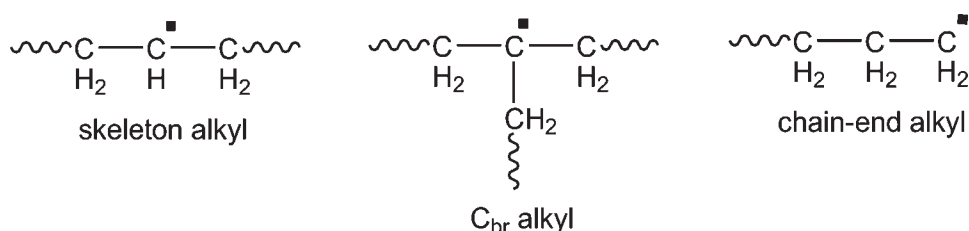


**Figure 8** Different alkyl configurations obtained via the photooxidative mechanism.

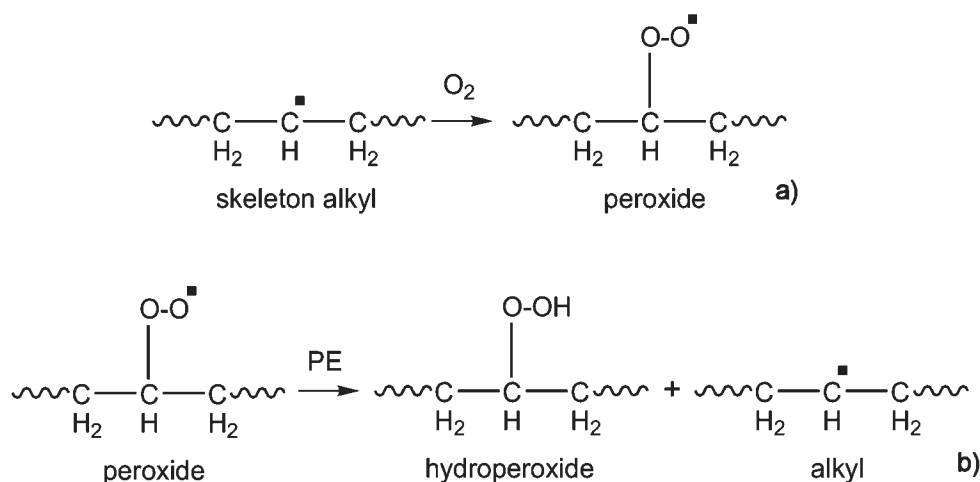


Figure 9 Formation of (a) peroxide and (b) hydroperoxide by reaction of oxygen with an alkyl site.

( $R^\bullet$ ) coming from the initial step of the photooxidation mechanism or via the reaction with a peroxide. Free radicals at the chain end can be relevant to the cleavage of C—C bonds in the main chains because their dissociation energy is about  $80 \text{ kcal mol}^{-1}$  and the quanta of energy provided by the solar light is sufficient to cause this breaking.<sup>30</sup>

So the rearrangement of the microstructure via the reaction of the free radicals has probably led to the formation of ethyl branches. One can reasonably imagine that this structure results from the combination of a free radical, coming from the abstraction of a hydrogen atom of a methylene group ( $CH_2$ ) separated by one carbon atom from a chain end methyl ( $CH_3$ ) group, with a radical provided by the cleavage of C—C bonds of a polymeric chain.

The presence of oxygen in the LDPE film, whose diffusion is favored by the long time elapsed during the nightly periods, is responsible of the polymer oxidation. However, the direct reaction between oxygen and polyethylene is nearly impossible. Only the sites that have been activated by a photon are susceptible to give significant oxidation kinetics.

Because a majority of these alkyl sites are of the skeleton type, the reaction leads primarily to peroxide as depicted in Figure 9(a). The peroxide itself is enough reactive to activate another chain, giving rise to a hydroperoxide and regenerating an alkyl radical, as shown in Figure 9(b).

Because the alkyl radicals are not detectable *per se* with the FTIR and NMR techniques utilized in this work, special experiments using Electron Spin Resonance should be necessary, as shown previously.<sup>31</sup> However, the absorption bands at  $3600 \text{ cm}^{-1}$  and around  $3500 \text{ cm}^{-1}$  observed by FTIR suggest the presence of hydroperoxides because these absorptions are generally attributed to the OH stretching of such groups.<sup>3,19,32</sup>

As shown previously in the literature the processes involving oxidized species are numerous and complex. Nevertheless, in a simplified model, it can be considered that their photochemical decomposition into free radicals plays an important role [Fig. 10(a)]. Within this scheme, the resulting alkoxy radicals produce an alcohol functions by reaction with a polyethylene chains [Fig. 10(b)].

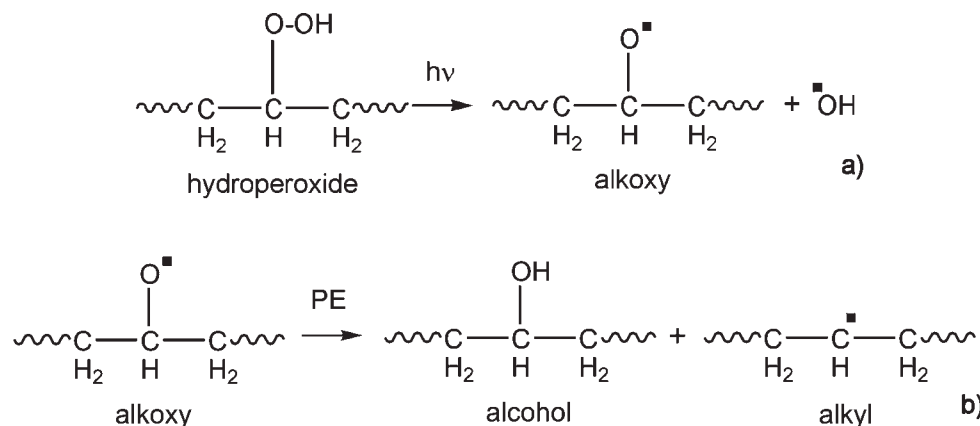
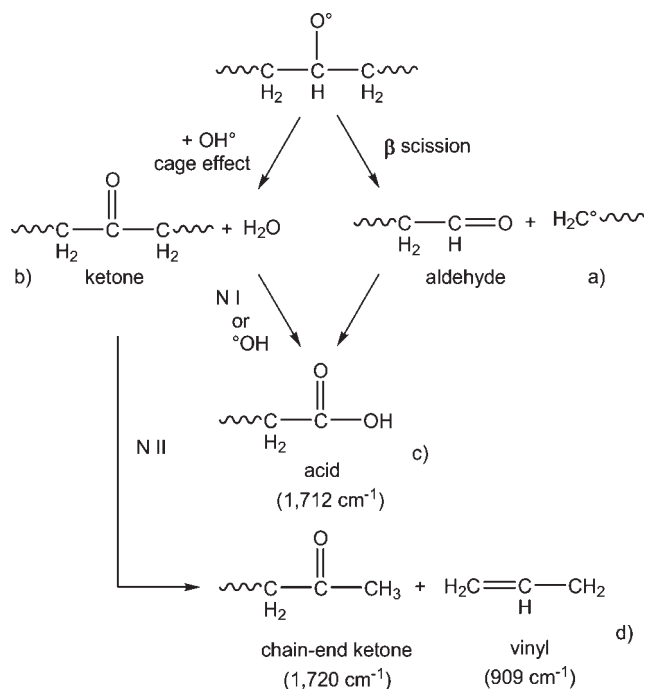


Figure 10 Formation of (a) alkoxy and (b) alcohol by reaction of oxygen with an alkyl site.



**Figure 11** (a) Formation of aldehyde via  $\beta$  scission. (b) Formation of ketone. (c,d) Alternative chain scission processes.

According to the literature, the process of chain scission results for a major part from the generation of hydroperoxides presented earlier. As such, they initiate a chain reaction of self-oxidation, leading to

the formation of  $-\text{OH}$  and mainly  $\text{C}=\text{O}$  groups. Temperature activates the  $\beta$  scission of the alkoxy radical leading to the apparition of an aldehyde and an alkyl radical [Fig. 11(a)]. Another route in hydroperoxides decomposition consists in the formation of ketone groups via the elimination of a small molecule of water [Fig. 11(b)].<sup>11</sup> Subsequently, the ketone undergoes a scission at a location neighboring the  $\text{C}=\text{O}$  group via the Norrish I process. The terminal ketone radical produced reacts with a  $[\text{chemp}]\text{OH}$  radical leading to the formation of a carboxylic acid (detectable by the FTIR line at  $1720\text{ cm}^{-1}$ ) [Fig. 11(c)]. Ketone groups may also lead to the formation of chain scissions by a second route [Fig. 11(d)]. In this case, the cut is produced via the Norrish II process at a location more distant to the  $\text{C}=\text{O}$  group. The shorter chains produced by this reaction present at their end a ketone group and a vinyl group ( $910\text{ cm}^{-1}$ ), respectively.

The production of crosslinks is also a complex process that can be activated by at least three different mechanisms. The first one, schematically represented in Figure 12(a), which is more active for short ageing times, results from the combination of a skeleton (secondary) alkyl radical with a vinylidene group. The former comes from photon activation. The latter is generally attributed to  $\beta$  scission of the polymer chain favored by thermomechanical degradation during processing.<sup>5,33</sup> It is present in the original LDPE film as proved by the evolution of the  $888\text{ cm}^{-1}$  FTIR

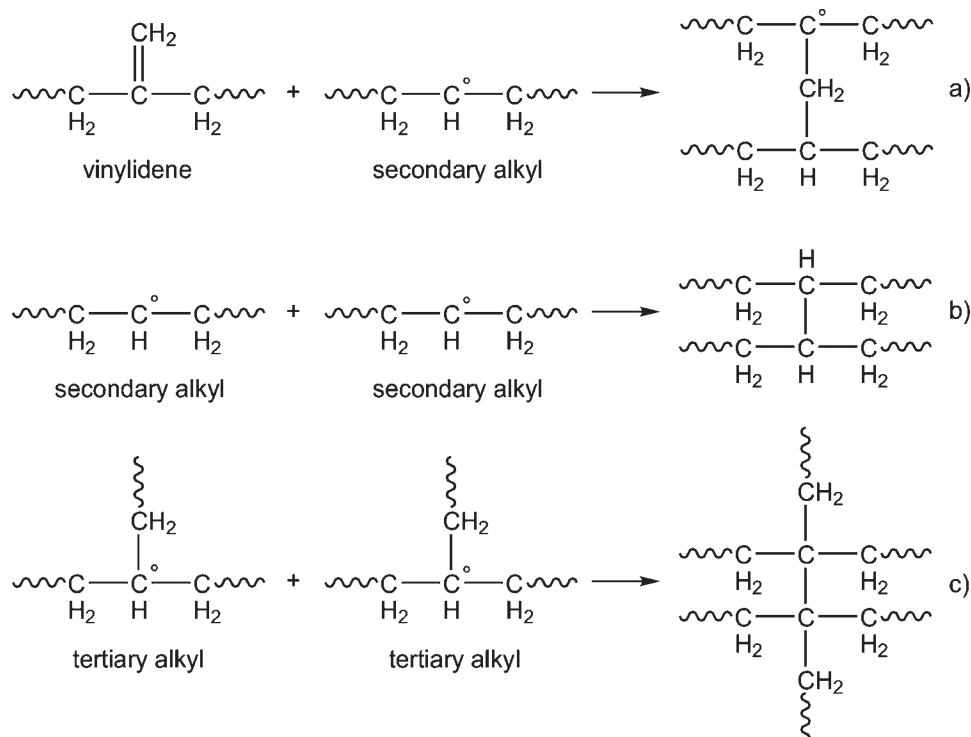


**Figure 12** Formation of a crosslink between two polyethylene chains via different mechanisms: (a) from a vinylidene group and a secondary alkyl radical, (b) from two secondary alkyl radicals and, (c) from two tertiary alkyl radicals.

band displayed in Figure 5. In this case, we obtain a junction in which the two polyethylene chains are connected by one intermediate  $\text{CH}_2$  group.

By contrast, in the second mechanism [Fig. 12(b)], the reacting species are two secondary alkyl radicals, both produced by chain oxidation process. The two chains are linked by a covalent bond between tertiary carbon atoms.

In the same way two tertiary radicals can also combine together to form another kind of junction made of quaternary atoms linked by a covalent bond [Fig. 12(c)]. As we saw in section "NMR Characterization" through the NMR peak at 38.81 ppm, the formation of such quaternary carbons is an effective but rather late process in LDPE.

### Influence of microstructural changes on the mechanical properties

The mechanical properties of polyethylene have been characterized and modeled by many authors and in particular by one of us.<sup>34,35</sup> It is now well understood that each phase in the semicrystalline microstructure plays an important role as in a nanocomposite material. On one hand, the crystalline lamellae behave like reinforcing particles whose elastic rigidity is considerable, notably along the chain axis. They are also capable to deform plastically through slip mechanisms, so that higher extension ratio can be imposed before failure. Furthermore, at large strain, a crystalline texture develops (the chain axis rotating toward the tensile direction), which induces an increasing hardening that stabilizes incipient plastic instabilities. On the other hand, the amorphous phase is present in the interstitial layers between the crystalline lamellae and forms the matrix of the nanocomposite morphology. The elastic modulus of the amorphous phase is typically that of a rubber (a few MPa) because the glass transition temperature is far below room temperature. The less crystalline grades of polyethylene are therefore those with the weakest Young's modulus. Furthermore, the role of the amorphous phase is important in the plastic stage and up to rupture through the following processes: (i) it accommodates the large strain inhomogeneities that develop among the crystallites due to the limited number of slip systems, thus making the yield point more gradual and avoiding brittle fracture, (ii) it undergoes significant microcavitation that consumes energy and avoids the propagation of dangerous microcracks, (iii) it participates to the strain hardening by the virtue of considerable chain orientation. The latter effect depends for a large part on the existence of tie molecules linking the individual lamellae, and also on the degree of branching that favors chain entanglement.

Considering the above factors, we interpret now more precisely the effect of climatic ageing on the

tensile behavior of LDPE. The evolution of the Young's modulus,  $E$ , is not a monotonous increase. In the first months of the ageing protocol, the increase is rapid. This stiffening is essentially controlled by the secondary crystallization of the amorphous chains whose mobility is enhanced by the chain scission processes.<sup>5,17,35</sup> Also, several authors proposed that the replacement of C—H bonds by C=O bonds during the oxidation of the amorphous regions introduces stronger intermolecular bonds and contributes to the modulus increase.<sup>9,31</sup> As for the crosslinking process, it does not play an important role on the elastic modulus at least during the first 3 months of oxidation.

As we saw in the experimental section, the weathering principally affects the capability of the material to undergo large plastic stretching. This embrittlement, which has a negative impact on the durability of LDPE films for their application in greenhouse covering, is principally attributed to the reduction of the average molecular weight caused by the multiplication of chain scissions.<sup>3,17,18,34</sup> The most probable cause of ductility loss in the plastic stage comes from the scission of tie molecules joining two adjacent crystallites, because it is known<sup>36,37</sup> that these particular chains play a major role in the cohesion of the material at large plastic strain. Inversely, the chain junctions produced by the crosslinking processes are likely to limit the decay of the tensile strength and to support a reasonable elongation at break for a longer ageing time. However, because we showed that a significant part of the crosslinks are formed from preexisting vinylidene groups [Fig. 12(a)], we propose that the drastic drop of the film ductility after 4 months ageing (Fig. 3) is due to the definitive exhaustion of the vinylidene groups revealed par the FTIR characterization in (Fig. 5) at about the same ageing time.

The presence of quaternary atoms revealed by NMR, accompanied by the increase of the tensile strength (Fig. 2), strongly suggest that crosslinking processes eventually occurred in the LDPE microstructure at the end of the aging protocol. However, these processes remain without significant incidence on the elongation at break since, at this stage of ageing, the reduction of the molecular weight is so important that the material has definitively lost its ductility.

### CONCLUSIONS

Climatic ageing of LDPE films for greenhouses covering in a sub-Saharan region leads to a rapid stiffening of the material accompanied by a loss of toughness. *In situ* climatic ageing experiments were performed to examine this effect quantitatively and



to correlate it to the microstructural changes induced by the weathering.

The characterization of the microstructure of the LDPE films by FTIR and  $^{13}\text{C}$  NMR revealed that the macromolecules are branched with numerous short chains. Butyl branches and secondary amyl branches have been identified. Also the initial microstructure includes many unsaturated chain defects, notably vinylidene groups.

During ageing, the formation of hydroperoxides plays a key role because it controls indirectly the chain scission process. The shorter chains generated, that are more mobile, favor the secondary crystallization and consequently induce an increase of the Young's modulus. Unfortunately, this process affects also the tie chains that are mainly in charge of maintaining the material cohesiveness at large stress. Consequently, the rapid multiplication of chain scissions is the main cause of embrittlement.

Crosslinking is another important process induced by climatic ageing of LDPE. Following current models proposed by previous authors, we have analyzed three mechanisms that lead to different kinds of chain junctions. The first one combines a vinylidene group and a skeleton alkyl, leading to junctions made of two tertiary carbons separated by a  $\text{CH}_2$  group. Because the vinylidene groups do not regenerate, this process is likely to saturate after some ageing time, typically 4 months. The two other crosslinking mechanisms, based on the reaction of secondary or tertiary alkyls, are also taken in account. They lead to junctions characterized by a covalent bond joining either tertiary or quaternary carbon atoms, respectively. All three crosslinking mechanisms are preferentially activated within the amorphous phase. The first one, arising from vinylidene consumption, saturates after 4 months ageing. The second one becomes prominent after this critical time. The third one, revealed by  $^{13}\text{C}$  NMR through the formation of quaternary carbon atoms, does not seem to be very active. Generally speaking, crosslinking limits the mechanical degradation due to chain scission. However, it is not sufficient to avoid the progressive decay of the films. This is due partly to the early exhaustion of vinylidene groups and partly to the insufficient generation of tertiary carbons. In consequence, sustainable use of LDPE films for greenhouses covering is impossible in the present state of the technology in sub-Saharan sites.

The authors are grateful to the different partners of this project, the University of Laghouat (in particular its past president Prof. Aïssa Benhorma) which favored the emergence of the research, the University of Bordeaux I (Dr. R. Huchon and Prof. B. de Jeso) which offered a favorable environment for the investigation of specimen microstructure and for stimulating discussion, and the Ecole des Mines de Nancy,

INPL (Dr. A. Dahoun and Mr. J. M. Hiver), which provided the final help to perform complementary experiments and conclude this publication.

## References

- Severini, F.; Gallo, R.; Ipsale, S.; Del Fanti, N. *Polym Degrad Stab* 1986, 14, 341.
- Severini, F.; Gallo, R.; Ipsale, S.; Del Fanti, N. *Polym Degrad Stab* 1987, 17, 57.
- Severini, F.; Gallo, R.; Ipsale, S. *Polym Degrad Stab* 1988, 22, 53.
- Basfar, A. A.; Idriss Ali, K. M. *Polym Degrad Stab* 2006, 91, 437.
- Mendes, L. C.; Rufino, E. S.; DePaula Filipe, O. C.; Torres, A. C. *Polym Degrad Stab* 2003, 79, 371.
- Gulmine, J. V.; Janissek, P. R.; Heise, H. M.; Akcelrud, L. *Polym Degrad Stab* 2003, 79, 385.
- Carrasco, F.; Pagès, P.; Pascual, S.; Colom, X. *Eur Polym Mater* 2001, 37, 1457.
- Hassini, N.; Guenachi, K.; Hamou, A.; Saiter, J. M.; Marais, S.; Beucher, E. *Polym Degrad Stab* 2002, 75, 247.
- Verdu, J., Ed. *Vieillessement Des Plastiques*; Eyrolles, Afnor: Paris, 1984.
- Fayolle, B.; Colin, X.; Audouin, L.; Verdu, J. *Polym Degrad Stab* 2007, 92, 231.
- Lemaire, J.; Arnaud, R.; Gardette, J. L. *Pure Appl Chem* 1983, 55, 1603.
- Gugumus, F. *Angew Makromol Chem* 1988, 158, 151.
- Gugumus, F. *Angew Makromol Chem* 1990, 176, 127.
- Gugumus, F. *Angew Makromol Chem* 1990, 182, 85.
- Tidjani, A. *Polym Degrad Stab* 2000, 68, 465.
- Chabira, S. F.; Huchon, R.; Sabaa, M. *J Appl Polym Sci* 2003, 90, 559.
- Chabira, S. F.; Sebaa, M.; Huchon, R.; De Jeso, B. *Polym Degrad Stab* 2006, 91, 1887.
- Qureshi, F. S.; Amin, M. B.; Maadhah, A. G.; Hamid, S. H. *Polym Plast Technol Eng* 1989, 28, 649.
- El Awady, M. M. *J Appl Polym Sci* 2003, 87, 2365.
- Wunderlich, B. *Macromolecular Physics, Vol. 1: Crystal Structure, Morphology, Defects*; Academic Press: New York, 1973.
- Silverstein, R. M.; Basler, R. C.; Morill, T. C., Eds. *Identification Spectrométrie De Composés Organiques*; De Boeck Université: Paris and Brussels, 1998.
- Birkinshaw, C.; Buggy, M.; Daly, S.; O'Neill, M. *Polym Degrad Stab* 1988, 22, 285.
- Bennett, R. L.; Keller, A.; Stejny, J.; Murray, M. *J Polym Sci Part A: Polym Chem* 1976, 14, 3027.
- Grenier-Loustalot, M. F. *J Polym Sci Part A: Polym Chem* 1983, 21, 2683.
- Freche, P.; Grenier-Loustalot, M. F. *Eur Polym Mater* 1984, 20, 31.
- Hansen, E. W.; Blom, R.; Bade, O. M. *Polymer* 1997, 38, 4295.
- Albert, C. F.; Busfield, W. K. *J Polym Sci Part A: Polym Chem* 1997, 35, 1549.
- Randall, J. C.; Zoepfl, F. J.; Silverman, J. *Makromol Chem Rapid Comm* 1983, 4, 149.
- Dilara, P. A.; Briassoulis, D. *Polym Test* 1998, 17, 549.
- Severini, F.; Gallo, R.; Ipsale, S. *Arab J Sci Eng* 1988, 13, 533.
- Nakamura, K.; Ogata, S.; Ikada, Y. *Biomaterials* 1998, 19, 2341.
- Torika, A.; Takeuchi, A.; Nagaya, S.; Fueki, K. *Polym Photochem* 1986, 7, 199.
- Severini, F.; Gallo, R. In *Handbook of Polymer Science and Technology, Composites and Specialty Applications*; Cheremisinoff, N. P., Ed.; CRC Press: New York, 1989; Vol. 4, Chapter 14, p 485.
- La Mantia, F. P.; Gardette, J. L. *Polym Degrad Stab* 2002, 75, 1.
- Sebaa, M.; Servens, C.; Pouyet, J. *J Appl Polym Sci* 1993, 47, 1897.
- G'sell, C.; Dahoun, A. *Mater Sci Eng A* 1994, 175, 183.
- Addiego, F.; Dahoun, A.; G'sell, C.; Hiver, J. M. *Polymer* 2006, 47, 4387.